PLoS one

Surface Modifications by Field Induced Diffusion

Martin Olsen*, Magnus Hummelgård, Håkan Olin

Department of Natural Sciences, Engineering and Mathematics, Mid Sweden University, Sundsvall, Sweden

Abstract

By applying a voltage pulse to a scanning tunneling microscope tip the surface under the tip will be modified. We have in this paper taken a closer look at the model of electric field induced surface diffusion of adatoms including the van der Waals force as a contribution in formations of a mound on a surface. The dipole moment of an adatom is the sum of the surface induced dipole moment (which is constant) and the dipole moment due to electric field polarisation which depends on the strength and polarity of the electric field. The electric field is analytically modelled by a point charge over an infinite conducting flat surface. From this we calculate the force that cause adatoms to migrate. The calculated force is small for voltage used, typical 1 pN, but due to thermal vibration adatoms are hopping on the surface and even a small net force can be significant in the drift of adatoms. In this way we obtain a novel formula for a polarity dependent threshold voltage for mound formation on the surface for positive tip. Knowing the voltage of the pulse we then can calculate the radius of the formed mound. A threshold electric field for mound formation of about 2 V/nm is calculated. In addition, we found that van der Waals force is of importance for shorter distances and its contribution to the radial force on the adatoms has to be considered for distances smaller than 1.5 nm for commonly used voltages.

Competing Interests: The authors have declared that no competing interests exist.

* E-mail: Martin.Olsen@miun.se

Introduction

A voltage pulse between a scanning tunneling microscope (STM) tip and a surface will modify the surface under the tip creating either a mound or a pit on the surface, see ref. [1,2] and Table 1.

The surface atoms on the tip or sample are subjected to an electrostatic force and this can lead to two different scenarios: either field evaporation [3–12] or field enhanced diffusion [4,13–16] of atoms. However, field evaporation as Tsong [4] and others [17] has pointed out, is less likely compared to diffusion for the low voltages used in the experiments. In field evaporation an electric field of 20–50 V/nm is required [18] while typical voltages use in these experiments are 1–5 V/nm. In field enhanced diffusion, surface atoms (adatoms) are hopping between equivalent equilibrium positions due to lattice vibrations [19,20], and if they posses dipole moments they may be attracted towards the tip by the inhomogeneous electric field between the tip and the surface making a mound.

At tunneling distances the van der Waals force is also of importance because it grows as the inverse fourth power of distance [21], see equation (5). However, this contribution has been little discussed in the literature [22]. The situation is complicated by the proximity between tip and sample, which is only about one nanometer when tunneling occur, that might lead to the formation of a neck between tip and sample [6,23,24]. At larger distances, however, we can neglect the neck formation mechanism [12].

The experimental results, summarized in Table 1, seems to be somewhat contradictory but can be understandable if considering the complexity of the system: different set of parameters make different mechanisms dominate. We have several parameters to take into consideration: 1) tip-to-surface distance, 2) tip radius, 3) applied voltage polarity and magnitude and 4) material in the tip and sample.

The *phase diagram* in fig. 1 is a schematic of the formation of mounds and pits using the tip-surface distance and the voltage as parameters. It is mainly constructed using ref. [5,12] and ref. [17]. For positive tip we get mounds, area A in the phase diagram of fig. 1. For negative tip mounds form at shorter distances, area B, while pits are formed at larger distances, area C. This diagram is consistent with the references in Table 1, except for ref. [10]. However, the possibility of transport of positive as well as negative ions may likely explain this disagreement; negative ions are transported from negative to positive electrode and vice versa [4].

In area A with positive tip, we obtain mounds, made up of sample material likely created by field enhanced surface diffusion of adatoms. The mounds created using positive tip are unstable lasting only an hour in the experiment of ref. [5]. Mayer *et al.* [14] made a computer simulation of such a field enhanced diffusion of adatoms under an STM tip. From our model (see below) on electric field induced diffusion we can calculate the threshold electric field for mound formation for area A: inserting equation (25) for the threshold voltage U_0 into equation (18) for the electric field E yields for $r = 0$ the threshold field for mound formation $E_0 = \mu/\alpha \approx 2$ V/nm.

In area B, at short distances and negative tip voltage, mounds made of tip materials are formed as found by Hsiao et al [5]. The transport of tip material is due to field enhanced diffusion on the tip toward the gap, leading to a neck formation, that result in a mound when retracting the tip [5]. If the applied voltages is increased high enough, field evaporation of tip material will instead occur [5].

Table 1. Mound or pit formation for different tip and surface materials and tip polarity.

Reference	Tip	Surface	Effect of negative tip	Effect of positive tip
Mamin (1990) [3]	Au	Au	Mound	Mound
Hsiao (1994) [5]	Au or Cu	Si	Au or Cu mound[1]	Non-metallic mound[1]
Bessho (1994) [9]	PtIr	Au	Pit	Mound
Mascher (1994) [8]	Au	Au	Pit[2]	Mound[2]
Chang (1995) [24]	Au, W, PtIr	Au	Mound, Crater[3]	Mound, Crater[3]
Kondo (1995) [17]	W or Pt	Various[4]	Pit	-
Ohi (1995) [12]	Au	Au	Pit, Mound[5]	Mound
Hu (1998) [7]	Al	Si	Mound	Mound
Mayer (1999) [14]	W	Au	Mound	-
Zhang (2001) [6]	Au	Au	Mound, Crater	Mound, Crater
Park (2002) [10]	Al	Si	Erasure of mound	Increased mound size
Park (2002) [10]	Au	Si	Incresed mound size	Erasure of mound
Fujita (2003) [11]	Ag	Si	Mound	Mound

[1]: Element determination by scanning Auger microprobe spectra.
[2]: For triangular voltage pulse. Rectangular pulse used elsewhere.
[3]: Nonconducting liquid between tip and surface.
[4]: Au, Ag, In, Si, Pt, W, C, SiO_2, MoS_2 or $Bi_2Sr_3CaCu_2O_x$.
[5]: Pit created at larger tip-surface distance, mound at smaller.
doi:10.1371/journal.pone.0030106.t001

In area C, the experiments by Kondo et al. [17,25] show a strong correlation between the threshold voltage for pit formation and the binding energy for ten different materials: for example Au with a binding energy of 3.8 eV has a threshold voltage of $U = 3.5$ V, while W with binding energy of 8.8 eV has $U = 8.7$ V. Their
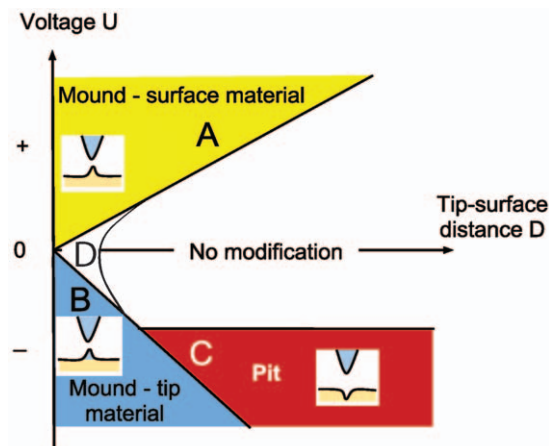

Figure 1. Phase diagram showing STM induced surface modifications at different tip voltage U and different tip-to-surface distance D mainly constructed using ref. [5,12] and ref. [17]. In drawing the lines for mound formation we have assumed that it is the electric field $E = U/D$ that decides if some particular kind of mound will be formed. Mounds will form at positive voltages, area A. From our model assuming field induced diffusion of adatoms we can calculate the threshold electric field for mound formation for area A to $E_0 = \mu/\alpha \approx 2$ V/nm. In area B we have transfer of tip materials to the surface making a mound of tip material on the surface. For pits, area C, we have assumed that they are formed at constant U independent of the tip-to-surface distance D in agreement with Kondo et al. [17]. At short distances and low electric fields, area D, the van der Waals force will contribute in creating a mound [22]. Close to the U-axis (not shown) at electrical fields above 20–50 V/nm field evaporation will occur [18].
doi:10.1371/journal.pone.0030106.g001

explanation for this mechanism is sublimation induced by tunneling electrons.

In area D, for short distances and low electric fields, Erts et al. [22] measured the force between a gold coated atomic force microscope (AFM) tip and a gold tip using an AFM cantilever placed inside a transmission electron microscope (TEM). They could in this way image the system while manipulating it. They found an anomalous high value of the jump-to-contact distance indicating a larger force than expected from the distances using the van der Waals force. Closer inspection revealed a thin neck formed between the tip and sample. Their interpretation was that the van der Waals force caused field induced surface diffusion leading to shorter gap which in turn increased the van der Waals force, and this avalanche of adatoms quickly formed the neck.

In this paper, we describe a field enhanced surface diffusion model (area A) and also a model at short distances and low electric fields where van der Waals forces are contributing (area D).

We develop a simple analytical model to calculate the static electric forces from the tip governing the motion of the adatoms. We extend the model of Mayer et al. [14] by including the surface induced dipole moment which introduces a force on the adatoms that depend on the polarity of the applied voltage between the tip and the surface. We find a novel formula for the threshold voltage for mound formation for positive tip as well as a relation between the mound radius and the applied voltage. In addition we include the van der Waals force described in ref [21,22]. We find that its contribution to the radial force on the adatoms is small for distances larger than 1.5 nm for commonly used voltages.

Analysis

Van der Waals force

In this section we will calculate the van der Waals interaction energy of an adatom with a parabolic tip, representing an STM tip, and thereafter the force. The (non retarded) van der Waals interaction energy between two atoms at distance s from each other is given by [21,26]

$$W(s) = -\frac{C}{s^6}. \qquad (1)$$

An approximate value of the constant C for identical atoms is given by $\hbar\omega_0\alpha^2$, see ref. [26], where $\hbar\omega_0$ is the energy of the strongest optical absorption line and α is the polarizability of the atoms. Following Israelachvili [21] we have for a ring-shaped element in the tip around the z-axis at radius r the volume $dV = 2\pi r dr dz$, see fig. 2. The number of atoms in the ring is then $dN = 2\pi r \rho dr dz$ where ρ is the number density of the tip material. The interaction energy between the ring and an adatom on the surface at $r = z = 0$ is then

$$dW = -\frac{2\pi C\rho r}{(r^2+z^2)^3} dr dz, \qquad (2)$$

using $s^2 = r^2 + z^2$. If the ring is a segment in a parabolic tip given by $r = \sqrt{2R(z-D)}$ with apex at $z = D$ and extending into infinity, the interaction energy for the adatom at $r = z = 0$ with the tip is

$$W = -\int_{z=D}^{z=\infty} \int_{r=0}^{r=\sqrt{2R(z-D)}} \frac{2\pi C\rho r}{(r^2+z^2)^3} dr dz. \qquad (3)$$

Integrating we obtain

$$W = -\frac{\pi C\rho}{6D^3}\left[1 - \frac{3Dd}{2B} - \frac{3D^3}{4B^{3/2}}\ln\left(\frac{d-\sqrt{B}}{d+\sqrt{B}}\right)\right], \qquad (4)$$

where $d = D + R$ and $B = d^2 - D^2$.

A plot of W as a function of R shows that it varies monotonically from $W = 0$ at $R = 0$ to $W = -\pi C\rho/(6D^3)$ as $R \to \infty$. The force *on the adatom* right under the tip is then $F = \frac{\partial W}{\partial D}$, so that the force is directed towards the tip. Using this equation (4) yields
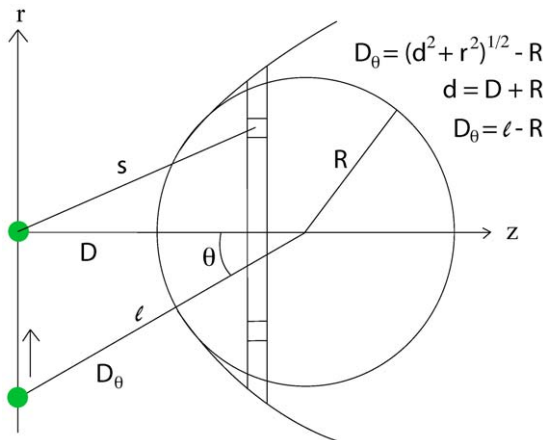

Figure 2. Calculation of van der Waals force on an adatom by a massive paraboloid tip with radius of curvature R at the apex. For a adatom sitting off-axis on the surface the distance to the tip is D_θ. The letters denoting distances, D, ℓ, D_θ, s and R are placed at the midpoint of the distances they represent.
doi:10.1371/journal.pone.0030106.g002

$$F = \frac{\pi C\rho}{2D^4}\left[1 - \frac{3Dd}{2B} + \frac{DR(2D^2+d^2)}{2B^2}\right.$$
$$\left. -\frac{3D^3}{4B^{3/2}}\left(1 - \frac{Rd}{B}\right)\ln\left(\frac{d-\sqrt{B}}{d+\sqrt{B}}\right)\right] = \qquad (5)$$
$$= \frac{\pi C\rho}{2D^4}\xi(D,R).$$

This equation can be used to calculate the van der Waals force on a adatom *right under the tip*. Plotting ξ in equation (5) as a function of D shows that it decreases monotonically from $\xi = 1$ at $D = 0$ towards zero as D approaches infinity. A plot of ξ as a function of R yields $\xi = 0$ at $R = 0$ and then increases monotonically towards $\xi = 1$ as R approaches infinity.

We now consider the van der Waals forces on the adatom when it is located on a conducting surface under the tip. The van der Waals force on an adatom *by the surface* is always perpendicular to the surface balancing the z-component of the force from the tip. To see how the adatom is moving it is thus more interesting to study the r-component. If we have the force $F(D_\theta)$ directed towards the center of the sphere approximating the parabolic tip, the force components on an adatom sitting off-axis on the surface are

$$F_z = F(D_\theta)\cos(\theta) = F(D_\theta)\frac{d}{\sqrt{d^2+r^2}}, \qquad (6)$$

$$F_r = -F(D_\theta)\sin(\theta) = -F(D_\theta)\frac{r}{\sqrt{d^2+r^2}}, \qquad (7)$$

where θ is the off-axis angle counted from the center of the sphere, see fig. 2. $F(D_\theta)$ is obtained from equation (5) by replacing D with the expression $D_\theta = \sqrt{d^2+r^2} - R$. This is the radial distance $\ell - R$ from the tip to the surface for an off-axis angle if the tip is approximately considered spherical seen from a point on the surface.

Approximating with $\xi = 1$ in (5) we obtain a simpler formula which yields a *upper limit* of the van der Waals force. The radial component becomes

$$|F_r| < \frac{\pi C\rho}{2(\sqrt{d^2+r^2}-R)^4}\frac{r}{\sqrt{d^2+r^2}}. \qquad (8)$$

Electrostatic dipole force

In this section we will calculate the static electric dipole force on an adatom when we have a voltage applied between the tip and the surface. To obtain a simple model we approximate the field as given by a point charge q located at a distance d over an infinite flat conducting surface. The midpoint of the adatom is located a distance z over the surface, see fig. 3. The potential Φ at a point is then given by

$$\Phi = \frac{q}{4\pi\varepsilon r_1} + \frac{-q}{4\pi\varepsilon r_2}, \qquad (9)$$

where we have $r_1 = \sqrt{(d-z)^2+r^2}$ and $r_2 = \sqrt{(d+z)^2+r^2}$. The first term is the potential due to the charge q and the second term is the potential due to the mirror of the charge q in the conducting

surface. $\varepsilon = \varepsilon_r \varepsilon_0$ is the permitivity of the medium between the charge and the surface. To obtain a useful model we must find an expression for the charge q as a function of the applied voltage U between the tip and the conducting surface. On the line connecting the charge q and its mirror $-q$ (i.e. $r=0$) we have at the distance r_1 from q:

$$\Phi(r_1) = \frac{q}{4\pi\varepsilon r_1} + \frac{-q}{4\pi\varepsilon(2d-r_1)}. \qquad (10)$$

We see from equation (10) that if $r_1 = d$, that is we are in the surface, we have $\Phi(d) = 0$. The voltage between the tip apex, at a distance R from q, and the surface is then given by $U = \Phi(R) - \Phi(d)$. So

$$\frac{q}{4\pi\varepsilon} = \frac{U}{2D}\left(R^2 + 2DR\right), \qquad (11)$$

using $d = D + R$.

We here assume as a model that the equivalent charge q is fixed at the center of curvature of the tip independent of the tip-to-surface distance D. This is only approximately true but leads to equation (18) that is true both in the limit of $D \ll R$ where we obtain $E = U/D$ and in the limit $R \ll D$ where we obtain $E \approx 0$.

We can now calculate q if we know U, D and R. $E_z = -\frac{\partial \Phi}{\partial z}$ and $E_r = -\frac{\partial \Phi}{\partial r}$ yields

$$E_z = -\frac{q(d-z)}{4\pi\varepsilon r_1^3} - \frac{q(d+z)}{4\pi\varepsilon r_2^3}, \qquad (12)$$

$$E_r = \frac{qr}{4\pi\varepsilon r_1^3} - \frac{qr}{4\pi\varepsilon r_2^3}, \qquad (13)$$

$$E_\phi = 0. \qquad (14)$$

Figure 3. Adatoms with dipole moments on the surface for $U > U_0$. The dipole moment $\bar{p} = \bar{\mu} + \alpha \bar{E}$ are tending to align to the strong field inside r_0 on the surface and points away from the surface outside r_0 where the field is weaker, see equation (20). The radial force on the dipole on the surface is due to this effect attractive inside r_0 and repulsive outside, tending to create a mound made of surface material with maximum radius r_0.
doi:10.1371/journal.pone.0030106.g003

It is interesting to study the field close to the surface, that is when $z \ll D$ (implying $z \ll d$). To do so we expand equation (12) and (13) in Taylor series around $z = 0$. We then obtain

$$E_z \approx -\frac{q}{4\pi\varepsilon}\left[\frac{2d}{(d^2+r^2)^{3/2}} + \frac{15d^3z^2}{(d^2+r^2)^{7/2}}\right], \qquad (15)$$

$$E_r \approx \frac{6qdr}{4\pi\varepsilon(d^2+r^2)^{5/2}}z. \qquad (16)$$

At $r = 0$ we have $E_r = 0$ because on the surface right under the charge by symmetry the only field component that exists is E_z. $E = \sqrt{E_z^2 + E_r^2}$. Dividing equation (16) with (15) we obtain

$$\frac{E_r}{E_z} \approx -\frac{3rz}{d^2+r^2}. \qquad (17)$$

Because r may be of about the same order as d and because we in the Taylor expansion have assumed that $z \ll d$ this quota is small compared to unity. Thus we may neglect E_r compared with E_z when calculating E. Using equation (11) in equation (15) for the z-component of the electrostatic field we then obtain in the surface (where $z = 0$) using $E \approx |E_z|$:

$$E \approx \left(1 - \frac{D^2}{d^2}\right)\frac{U/D}{\left(1 + \frac{r^2}{d^2}\right)^{3/2}}. \qquad (18)$$

The dipole moment $\bar{p}$ for an adatom in an electric field $\bar{E}$ is given by Tsong and Kellogg [20]:

$$\bar{p} = \bar{\mu} + \alpha\bar{E} + \frac{1}{6}\gamma\bar{E}^3 + \cdots, \qquad (19)$$

where $\bar{\mu}$ is the surface-induced dipole moment of the adatom, α is its polarizability and γ is its hyperpolarizability. $\bar{\mu}$ always points away from the surface that it sits on, see ref. [27,28], so μ is always positive in our calculations regardless of the polarity of the voltage U. We have for the $z-$ and $r-$components of the dipole moment $\bar{p}$, neglecting the hyperpolarizability term:

$$p_z = \mu + \alpha E_z, \qquad p_r = \alpha E_r, \qquad (20)$$

where μ is positive. p_z and p_r may therefore be positive or negative. The force on a dipole in an electric field is

$$\bar{F} = (\bar{p} \cdot \nabla)\bar{E}. \qquad (21)$$

Using equation (11), (20) and (15)–(16) and their derivatives into equation (21) we obtain to order z

$$F_z \approx \alpha\left[\frac{U}{2D}\left(R^2 + 2DR\right)\right]^2 \frac{60d^4 + 36d^2r^2}{(d^2+r^2)^5}z$$
$$-\mu\left[\frac{U}{2D}\left(R^2 + 2DR\right)\right]\frac{30d^3}{(d^2+r^2)^{7/2}}z, \qquad (22)$$

$$F_r \approx -\alpha \left[\frac{U}{2D} \left(R^2 + 2DR \right) \right]^2 \frac{12d^2 r}{(d^2 + r^2)^4}$$
$$+ \mu \left[\frac{U}{2D} \left(R^2 + 2DR \right) \right] \frac{6dr}{(d^2 + r^2)^{5/2}} . \qquad (23)$$

where z is the height over the surface for the center of the adatom, about one adatom radius. The distance z are only affecting F_z, not F_r, as we see from equations (22) and (23). We are now able to calculate the electrostatic forces on the adatom on the surface under the tip. The calculation above is valid for the first step in the mound formation where the surface still may be considered as flat. Mayer *et al.* [14] use $\mu = 0$ in their model so they do not obtain the polarity dependence.

Results and Discussion

To calculate the force we need to estimate the surface-induced dipole moment and the polarizability of an adatom. For metal atoms we have $\mu = 0.3 - 0.7$ Debye and $\alpha = 4 - 10$ Å^3, see ref. [20]. We use the average values $\mu = 0.5$ Debye and $\alpha = 7$ Å^3. Using SI-units this is $\mu = 1.7 \times 10^{-30}$ Cm and $\alpha = 7.8 \times 10^{-40}$ Cm^2/V. We assume that the adatom is a gold atom with a center height over the surface of about an atomic radius of gold so $z = 0.14$ nm. Atoms are detaching from steps on the substrate and becomes adatoms [14]. In this paper we only assume that the adatoms are on the surface and calculate how they move.

If a dipole in a inhomogeneous electric field is free to rotate or is created due to polarization by an electric field, the dipole is always attracted towards stronger field i.e $-F_r$ is positive. But the component of the dipole moment which is due to surface induction $\overline{\mu}$ always *points away* from the surface[27,28], making the electric force in equation (23) repulsive at some voltages and distances. This means that we may have an attractive force from the center under the tip out to some equilibrium radius where the force change sign and becomes repulsive. The force calculated from (23) is small for the commonly used voltage and distances, of order of 1 pN, see fig. 4, fig. 5 and fig. 6, but because the adatoms are hopping on the surface due to thermal vibration even a small net force can be significant in the drift of adatoms [19,20]. Setting $F_r = 0$ in equation (23) then yields
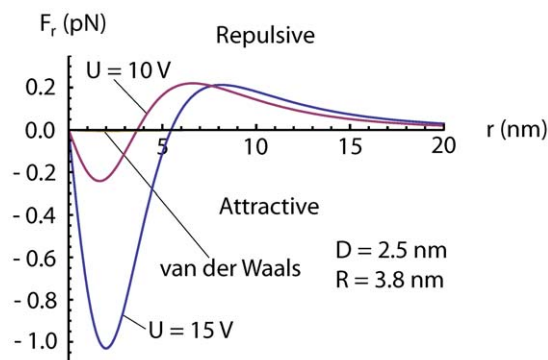

Figure 4. Radial dipole force on an adatom obtained from equation (23)using $D = 2.5$ nm and $R = 3.8$ nm and our values of μ and α for two different voltages $U > U_0 = 6.5$ V. Increasing all the distances D, R and r and the voltage U by a factor of 10 yields a reduction of the force F_r to 1/10. The radial van der Waals force calculated using equation (7) is barely visible in the figure at this "large" $D = 2.5$ nm.
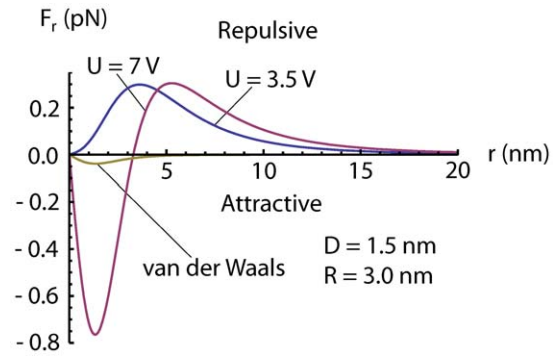doi:10.1371/journal.pone.0030106.g004

Figure 5. Radial dipole force on an adatom obtained from equation (23) using $D = 1.5$ nm and $R = 3.0$ nm and our values of μ and α for two different voltages U, one above and one below $U_0 = 3.7$ V. The van der Waals force has been calculated using equation (7) and plotted in the figure using $D = 1.5$ nm. For $D < 1.5$ nm the van der Waals force becomes important for the radial force on the adatoms.
doi:10.1371/journal.pone.0030106.g005

$$r_0 = (D + R) \sqrt{ \left(\frac{U}{U_0} \right)^{2/3} - 1}, \qquad (24)$$

where

$$U_0 = \frac{\mu D (D + R)^2}{\alpha R (2D + R)} . \qquad (25)$$

Using for example $D = 1.5$ nm and $R = 3$ nm we obtain $U_0 = 3.7$ V. r_0 is the equilibrium radius on the surface at voltage $U > U_0$ where the force changes sign from attractive to repulsive as we are moving out from the center right under the tip towards infinity, see fig. 3. For voltages U between zero and U_0 the electrostatic force is repulsive for all distances r, that is there is no equilibrium distance.

Inserting equation (25) for the threshold voltage U_0 into equation (18) for the electric field E yields for $r = 0$ (a small mound with radius zero is barely formed according to the definition of threshold
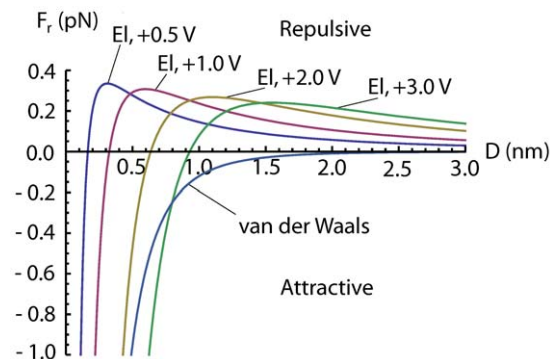

Figure 6. Radial van der Waals force from equation (7) and radial electric forces (El) from equation (23) for different tip voltages, at $r = (R + D)/2$ as a function of tip-to-surface distance D. $R = 3$ nm.
doi:10.1371/journal.pone.0030106.g006

5

voltage, equation (24)) the threshold field for mound formation $E_0 = \mu/\alpha \approx 2$ V/nm.

We have thus two novel findings for positive tip voltages: a threshold field for mound formation of about 2 V/nm and a voltage dependent radius of the mound, equation (24).

For negative voltages, in contrast to positive voltages, the force F_r is attractive for all distances, except at $r = 0$ where the force is zero, as we see from equation (23), so negative voltage is tending to creating a mound on the surface with no threshold voltage. This due to that in this case the dipole moment p_z does not change sign at a certain field as we have at positive tip.

The experimental findings are somewhat contradictory: a more or less sign independent threshold voltage of about 3.5 V is observed according to ref. [3,24]. However, mound formation is less reproducible with positive voltage at the tip [11,24]. A mound created by a tip-positive pulse could be removed by applying a negative pulse in some cases [9]. Using a gold (copper) tip over a silicon surface, a negative voltage on the tip yields a gold (copper) mound on the surface, but for positive voltage the mound are not made up of metal [5]. This indicates that at negative tip, materials from the tip are transferred to the surface while at positive tip surface material are attracted towards the area under the tip creating a mound. Using a gold tip and a gold surface, at high tunneling resistance (large tip to surface distance) at a negative tip a hole was created and at positive tip a mound was created [12].

However, at low tunneling resistance (small tip to surface distance) a mound adjacent to a pit was often created by a negative tip where the current kept flowing even after the voltage pulse, indicating necking between surface and tip [12]. Transfer of material between tip and surface seems to be possible both ways depending on the materials used, see ref. [10] and table 1.

Mayer et al. [14] simulated the diffusion of adatoms on a surface using $D = 25$ nm, $R = 38$ nm and $U = -100$ V at the tip. (They also measured experimentally the size of a mound while it was growing under the tip.) They obtained a mound diameter (at which the growth rate is zero) of 40 nm. Their simulation model was independent of the sign of the voltage so $U = +100$ V would have given the same result. To compare this with our model we calculate the threshold voltage using equation (25) in our paper and the R and D in the simulation using our estimate $\mu = 1.7 \times 10^{-30}$ Cm and $\alpha = 7.8 \times 10^{-40}$ Cm^2/V for a metal adatom. We then obtain $U_0 = 65$ V. Thereafter we calculate the equilibrium radius at $U = 100$ V using (24). We then obtain a radius of $r_0 = 36$ nm in good agreement with the simulation result. However, this should be a coincidence because the mechanisms are different in the two cases.

r_0 is the maximum radius of the mound in our model because no adatoms can be attracted from outside of this radius. In the simulation made by Mayer et al. adatoms are attracted from all radius making the mound thickness grow inside some radius etching away surface material outside this radius. The similar results though increases the reasonability of our approach to the field induced diffusion model.

Calculating the van der Waals force, we find that it is relatively small compared to the dipole force for distances larger than $D = 1.5$ nm using voltages commonly used in experiments. However, at small distances the van der Waals force will dominate over the electrostatic dipole force [22,29], see fig. 4, fig. 5 and fig. 6. For the van der Waals force we have $C = 1.89 \times 10^{-77}$ Jm^6, see ref. [21], and the number density of the material in the tip is estimated as $\rho = 5.86 \times 10^{28} m^{-3}$ yielding the value of the factor $\frac{\pi C \rho}{2D^4} = 1.7$ pN for $D = 1$ nm in equation (5). The radial component on an off-axis adatom will be smaller than this

according to equation (7). An upper limit for the radial van der Waals force is given by equation (8). Van der Waals induced surface diffusion dominates for this small distances for commonly used voltages. This effect may explain the neck formation obtained by Erts et al., [22], see text for area D in the introduction. The effect of adding the radial van der Waals force to the dipole force is that it tends to lower the threshold voltage for mound formation at positive tip making the mounds larger at a given applied voltage.

Other effects that may influence the mound formation is charge disorder effects, dipole-dipole interaction and dislocation activity which we will discuss below. Charge disorder interactions, where we have fluctuation-induced interaction between randomly charged dielectrics, is considered by ref. [30,31]. At larger distances this effect can dominate over the van der Waals force. How does this affect the mound formation? A length scale for the total force f as a function of the distance D is the Bjerrum length, $\ell_B = e^2/(4\pi\varepsilon_0 k_B T) \approx 56.8$ nm at room temperature, see [31]. We see from fig. 2 in [31] that for our distances D, about 1–50 nm, we have for quenched charge disorder $f/f_{vdW} \approx 1$ that is, the van der Waals force is dominating. For annealed charge disorder they obtain f/f_{vdW} between 1 and 1.6 for all distances so even here is the total force of the same order as of the van der Waals force. Thus for our distances charge disorder effects can be neglected when the van der Waals force can be neglected. The dipole-dipole interaction between adatoms on the surface should be less important because their interaction should seem to average out. This due to that the adatoms position on the surface are random so their average behaviour would mainly be determined by the field from the tip. Changes in temperature should only effect the diffusion rate [19] but not the equilibrium radius r_0 because it does not affect the force F_r which is given by the electric field. Recently, Mordehai et al. [32] finds, using a molecular dynamics simulation, that jump-to-contact between nanoparticles likely is due to dislocation activity. The particles are initially dislocation free and are in this state even after the jump-to-contact, they call this pseudoelasticity. This process is according to the simulation faster than competing processes like surface diffusion and may play a role in the formation of a mound in area D in fig. 1.

To test our model, one way would be to measure the mound radius as a function of applied voltage for tip-positive voltage pulse. In the literature we have only seen this experiment done for a negative tip, see Fujita et al. [11]. The lacking of experimental data for positive tip might be due to the experimental difficulty to reproduce mound formation for this tip polarity [11,24].

If one wants to create mounds on a surface, using negative tip is probably more effective. The mounds seems then be made up by tip material which may make the mounds more stable [5] than mounds constructed of surface material using a positive tip. However, for dynamic use in electronics we may not want the mound to be stable. Because the size of the mound for positive tip is limited by r_0 the mound formation may be more controlled in this case than at negative tip where we may have unrestricted growth of the mound trying to bridge the gap between tip and surface.

The same type of behaviour that we see on the surface under a STM-tip we may have on the tip itself, with mound formation above a threshold voltage. If we have two electrodes of different shape (tip radius) and material the threshold voltage for mound formation may be different on the two electrodes. By choosing a material with low mobility of adatoms as one electrode we may prevent mound formation on this electrode.

A way to monitor most of the parameters directly is to do the experiment using an STM inside a transmission electron microscope (TEM) where one can image the tip-surface system while
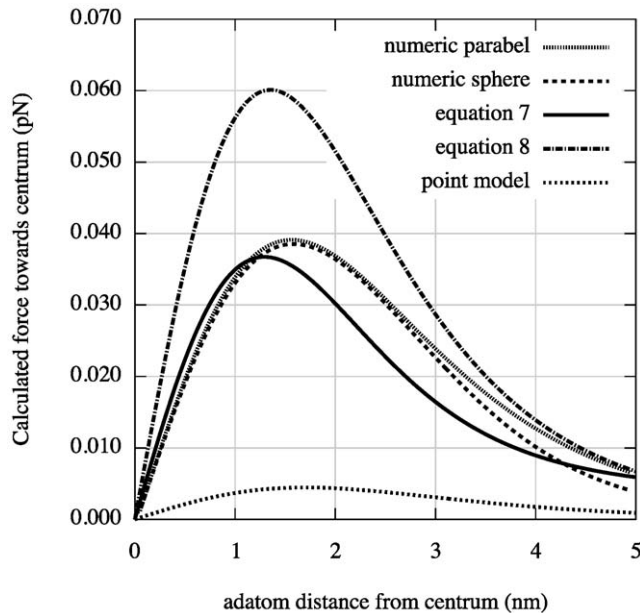
Figure 7. Radial van der Waals force on an adatom from simulations of a parabolic and a spherical tip respectively as a function of the distance r from the centrum under the tip to the adatom using numerical integration of equation (1). Also plotted in the figure is equation (7) and (8). $D = 1.5$ nm and $R = 3$ nm. Even the curve of a point model has been added. We see that equation (7) agrees well with the simulated curves close under the tip but underestimates the van der Waals force somewhat for larger r where the approximation of the tip as a sphere becomes too crude. The simpler formula equation (8) assuming $\xi = 1$ overestimates the force compared with the simulations in the figure. However, even this equation should underestimate the force for even larger r because the assumption of the tip as a sphere that both equation (7) and (8) uses breaks down. That the simulated value for the parabolic tip tend to sink below the curve from equation (8) at $r = 5$ nm is probably due to the limited size of the tip used in the simulation. In deriving equation (5), that equation (7) and (8) uses, we assume that the tip is extended to infinity.
doi:10.1371/journal.pone.0030106.g007

manipulating it [33,34]. All important parameters are accessible by TEM imaging: the tip-surface distance, tip radius, movement of tip or sample material, while the STM provide tip motion and bias voltage. In a TEM one also may see that the effective radius can be smaller than expected because there are often small asperities sitting on the large tip close to the surface [22].

The findings in this paper is not only of importance to understand the formation of structures under the STM tip, but may also be of importance in electronics applications for example recently described in ref. [16], where a temporary mound seems to be created between electrodes during a voltage pulse reducing (but not bridging) the gap and thus reducing tunneling resistance several orders of magnitude. Different resistance values can then be interpreted as digital ones and zeroes.

Another application that could be of importance is sintering of nanoparticles for use in printed electronics [35]. The ink used for defining conducting paths consists of nanoparticles that need to be sintered to achieve high enough conductivity. One method is
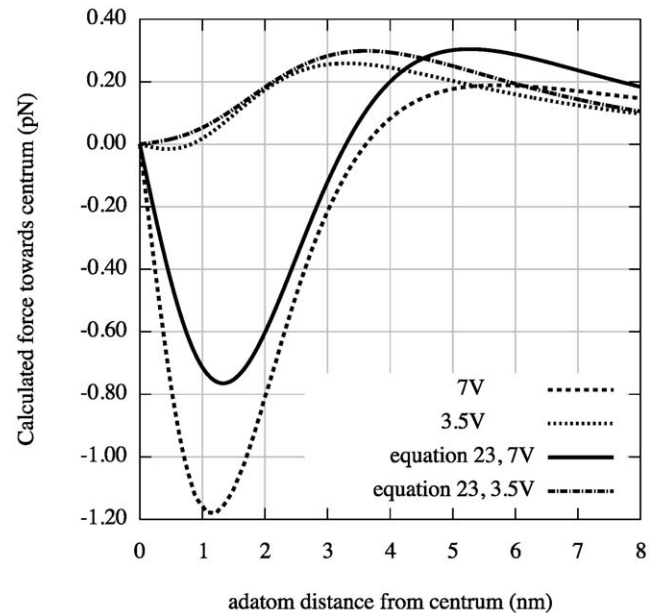
Figure 8. Radial dipole force on an adatom simulated using a conducting parabolic tip over a conducting plane for $U = 3.5$ V and $U = 7$ V respectively. Radius of curvature of the tip is $R = 3$ nm and tip-to-surface distance $D = 1.5$ nm. To calculate the electric field 400 positive charges are placed on the tip and 400 negative charges are placed on the surface. They are free to move and do so until they have reached their equilibrium positions. Thereafter the field generated by them is calculated and finally the radial force on the adatom. Also plotted is equation (23) for the same two voltages as above.
doi:10.1371/journal.pone.0030106.g008

electrical sintering [35,36] and to model this both the electrical and van der Waals induced surface diffusion models in this paper should be of relevance.

We have in this paper considered the static electric- and van der Waals forces on adatoms on a surface under a scanning tunneling microscope tip. We have described an analytical model of this system with three main conclusions: 1) the van der Waals force becomes important for tip-to-surface distances shorter than about 1.5 nm, 2) there is a threshold voltage in mound formation corresponding to a threshold electric field of about 2 V/nm, 3) and there is a relation between applied positive voltage and radius of the mound. To illustrate the result of our analysis we made plots. A plot of F_r from equation (7) as a function of r is shown in fig. 4 and fig. 5 and F_r as a function of D is shown in fig. 6. To verify the van der Waals-model we made simulations. We numerically integrated the van der Waals force given by equation (1) for a parabolic and spherical tip respectively, see fig. 7. In the figure we have also plotted equation (7) and (8). To test the model for the electrostatic dipole force we made a simulation of an adatom on a conducting plane under a conducting parabolic tip. This result is compared to equation (23) in fig. 8.

Author Contributions

Wrote the paper: MO MH HO.

References

1. Nyffenegger RM, Penner RM (1997) Nanometer-scale surface modification using the scanning probe microscope: Progress since 1991. Chem Rev 97: 1195–1230.
2. Tseng AA, Notargiacomo A, Chen TP (2005) Nanofabrication by scanning probe microscope lithography: A review. J Vac Sci Technol B 23: 877–894.
3. Mamin HJ, Guethner PH, Rugar D (1990) Atomic emission from a gold scanning-tunnelingmicroscope tip. Phys Rev Lett 65: 2418–2421.
4. Tsong TT (1991) Effects of an electric field in atomic manipulations. Phys Rev B 44: 13703–13710.

5. Hsiao GS, Penner RM, Kingsley J (1994) Deposition of metal nanostructures onto si(111) surfaces by field evaporation in a scanning tunneling microscope. Appl Phys Lett 64: 1350–1352.

6. Zhang HL, Li HL, Liu ZF (2002) Study on the delicate nanostructures formed on au(111) by scanning tunneling microscopy (stm). Microelectronic engineering 63: 381–389.

7. Hu X, von Blackenhagen P (1998) Generation and analysis of nano-scale al islands by stm. Appl Phys A 66: 707–710.

8. Mascher C, Damaschke B (1994) Creation of nanometer-scale structures with the scanning tunneling microscope. J Appl Phys 75: 5438–5440.

9. Bessho K, Hashimoto S (1994) Fabricating nanoscale structures on au surface with scanning tunneling microscope. Appl Phys Lett 65: 2142–2144.

10. Park JY, Phaneuf RJ (2002) Polarity dependence in pulsed scanning tunneling microscopy fabrication and modification of metal nanodots on silicon. J Appl Phys 92: 2139–2143.

11. Fujita D, Kumakura T (2003) Reproducible fabrication of metallic silver nanostructures on a si(111)-(7×7) surface by tip-material transfer of a scanning tunneling microscope. Appl Phys Lett 82: 2329–2331.

12. Ohi A, Mizutani W, Tokumoto H (1995) Nanometer-scale modifications of gold surfaces by scanning tunneling microscopy. J Vac Sci Technol B 13: 1252–1256.

13. Girard C, Joachim C, Chavy C, Sautet P (1993) The electric field under a STM tip apex: implications for adsorbate manipulation. Surf Sci 282: 400–410.

14. Mayer TM, Houston JE, Franklin GE, Erchak AA, Michalske TA (1999) Electric field induced surface modification of au. J Appl Phys 85: 8170–8177.

15. Mendez J, Gomez-Herrero J, Pascual JI, Saenz JJ, Soler JM, et al. (1996) Diffusion of atoms on au(111) by electric field gradient in scanning tunneling microscopy. J Vac Sci Technol B 14: 1145–1148.

16. Naitoh Y, Suga H, Horikawa M (2011) Physical model for high-to-low resistive switching of gold nanogap junction. Jpn J Appl Phys 50: 06GF10.

17. Kondo S, Heike S, Lutwyche M, Wada Y (1995) Surface modification mechanism of materials with scanning tunneling microscope. J Appl Phys 78: 155–160.

18. Tsong TT (1990) Atom-probe field ion microscopy: field ion emission and surfaces and interfaces at atomic resolution Cambridge University Press.

19. Kürpick U, Kara A, Rahman TS (1997) Role of lattice vibrations in adatom diffusion. Phys Rev Lett 78: 1086–1089.

20. Tsong TT, Kellogg G (1975) Direct observation of directional walk of single adatoms and adatom polarizability. Phys Rev B 12: 1343–1353.

21. Israelachvili JN (1992) Intermolecular and Surface Forces. Academic press limited.

22. Erts D, Lohmus A, Lohmus R, Olin H, Pokropivny AV, et al. (2002) Force interactions and adhesion of gold contacts using a combined atomic force microscope and transmission electron microscope. Appl Surf Sci 188: 460–466.

23. Pascual JI, Mendez J, Gomez-Herrero J, Baro AM, Garcia N, et al. (1993) Quantum contact in gold nanostructures by scanning tunneling microscopy. Phys Rev Lett 71: 1852–1855.

24. Chang TC, Chang CS, Lin HN, Tsong TT (1995) Creation of nanostructures on gold surfaces in nonconducting liquid. Appl Phys Lett 67: 903–905.

25. Kondo S, Lutwyche M, Wada Y (1993) Nanofabrication of layered materials with the scanning tunneling microscope. Appl Surf Sci 75: 39–44.

26. Kittel C (2005) Introduction to Solid State Physics - 8th ed John Wiley and Sons.

27. Linder B, Kromhout RA (1976) Dipoles induced by physical adsorption. Phys Rev B 13: 1532–1535.

28. Grossel P, Vigoureux JM, van Labeke D (1983) Static dipole moment of an atom or a centrocymmetric molecule near a perfect metallic surface. Phys Rev A 28: 524–531.

29. Erts D, Olin H, Ryen L, Olsson E, Thölen A (2000) Maxwell and sharwin conductance in gold point contacts investigated using tem-stm. Phys Rev B 61: 12725–12727.

30. Podgornik R, Naji A (2006) Electrostatic disorder-induced interactions in inhomogenous dielectrics. Europhys Lett 74: 712.

31. Naji A, Dean DS, Sarabadani J, Horgan RR, Podgornik R (2010) Fluctuation-induced interaction between randomly charged dielectrics. Phys Rev Lett 104: 060601.

32. Mordehai D, Rabkin E, Srolovitz DJ (2011) Pseudoelastic deformation during nanoscale adhesive contact formation. Phys Rev Lett 107: 096101.

33. Svensson K, Jompol Y, Olin H, Olsson E (2003) Compact design of a transmission electron microscope-scanning tunneling microscope holder with three-dimensional coarse motion. Rev Sci Instr 74: 4945–4947.

34. Nafari A, Angenete J, Svensson K, Sanz-Velasco A, Olin H (2011) Combining scanning probe microscopy and transmission electron microscopy. In: Bhushan B, ed. Scanning Probe Microscopy in Nanoscience and Nanotechnology 2. Springer Berlin Heidelberg: NanoScience and Technology. pp 59–99.

35. Hummelgård M, Zhang R, Nilsson HE, Olin H (2011) Electrical sintering of silver nanopartikle ink studied by in-situ tem probing. PloS ONE 6: e17209.

36. Allen ML, Aronniemi M, Mattila T, Alastalo A, Ojanperä K, et al. (2008) Electrical sintering of nanoparticle structures. Nanotechnology 19: 175201.